MIXED MODE DELAMINATION OF MULTIDIRECTIONAL CARBON FIBRE/EPOXY LAMINATES

N. Svensson
Pelmatic Consulting Engineers, F O Petersons gata 28, SE42131, Västra Frölunda, Sweden

M. D. Gilchrist*
Mechanical Engineering Department, University College Dublin, Belfield, Dublin 4, Ireland

SUMMARY

Scanning electron microscopy was used to identify fractographic features that are characteristic of different modes of interlaminar fracture. The cusp angle and the amount of fibre pull-out on the fracture surface can be used to characterise the different loading modes. A large amount of fibre pull-out is the dominant feature of a mode I fracture whilst in mode II large cusp angles and many cusps are the main characteristics. The amount of fibre pull-out, and subsequently broken fibres, per unit area was investigated and found to vary in proportion to the degree of mode I loading. Such methods can be used to analyse failure and the propagation of delamination in structural components. The energy associated with cusp formation constitutes a large proportion of the mode II fracture toughness component whilst the amount of fibre pull-out and fracture has a considerable influence on the mode I fracture component. The cusp angle was seen to provide a quantitative measure of the fracture surface roughness. A failure criterion which takes the fracture surface appearance into account was evaluated. The cusp angle was subsequently used to modify this failure criterion. As a consequence, this provided an improved agreement with the experimental data.

NOMENCLATURE

DCB	Double Cantilever Beam
ENF	End Notched Flexure
ELS	End Loaded Split
FRMM	Fixed Ratio Mixed Mode
MMB	Mixed Mode Bending
SEM	Scanning Electron Microscopy

INTRODUCTION

This particular project has concentrated on fractographic characteristics of delamination in multidirectional laminates and the influence of their formation on the apparent fracture toughness of the laminates. Particular features of interest were the cusp angle and the amount of fibre pull-out. Fracture surfaces from coupons tested under different known modes of loading were examined. These known modes of loading were obtained by testing standard fracture mechanics specimens (Double Cantilever Beam (DCB) for mode I tests[1,2], End Loaded Split (ELS) for mode II tests[3,4,5], Fixed Ratio Mixed Mode (FRMM) for mixed mode ratio I:II=4:3 tests[3,4,5] and Mixed Mode Bending (MMB) which can be used for any mixed mode loading ratio[6]) under both static and fatigue loading. The material examined was a carbon fibre/epoxy composite that is manufactured by Ciba Composites (T300/914).

Fracture toughness

A fracture mechanics approach is commonly used for modelling both catastrophic and slow growth delaminations in composite structures. The resistance to interlaminar crack growth is expressed by the material fracture toughness, designated G_C. Its general definition is the energy required to create new fracture surface areas, i.e. to propagate a crack from an

inherent defect. Crack propagation can occur in a combination of three different modes: I (tensile opening or peel), II (sliding shear) and III (tearing shear). The fracture toughness in each mode is denoted G_{Ic}, G_{IIc} and G_{IIIc} respectively. Fracture mechanics is more satisfactorily characterised using strain energy release rate (i.e., G) concepts than stress intensity factor (i.e., K) concepts. A number of composites were examined by Harris et al.[7] to provide comparative data of tensile strength and toughness (K_{Ic}) for fibre composites. The authors found a very simple relationship between the two properties which was independent of composition and manufacturing process which they thought very unlikely. They therefore concluded that the stress intensity factor, K_{Ic}, was an inappropriate parameter for characterising composites due to their heterogeneity and anisotropy. G is considered to be more suitable since it is based on global strain energy rather than local stress conditions at a crack tip.

Failure mechanisms

A delamination is constrained to grow between laminae due to the presence of fibres above and below the ply interface[8]. Sato et al.[9] reported the failure sequence for delamination failure during three point bending of unidirectional carbon fibre/epoxy from in-situ Scanning Electron Microscopy (SEM) and Acoustic Emission (AE) experiments. Fibre breakage began at about 60% of the ultimate failure load of the specimen as determined by the use of AE. Plastic deformation occurred from the broken fibre tip and along its sides followed by matrix cracking in the plastic region. A partial delamination was formed just before failure originating from the fibre breakage and matrix cracking and catastrophic crack propagation occurred from the delamination.

When interfacial failure occurs and a mode I component of load is present, fibre pull-out may occur. Due to debonding, fibres will bridge the wake of the crack and then eventually break when the induced bending stresses exceed the fibre strength. The reason for the fibre bridging is the misalignment of fibres across the plane of crack propagation. Fibre bridging contributes considerably to the measured fracture toughness of the specimen and Hu and Mai[10] have derived differential equations for the influence of fibre bridging on G_{Ic}. Fibre breakage does not occur as easily in ductile resins which lead to the formation of a bridged zone behind the crack tip which consequently helps to increase the toughness of the material[11]. The amount of fibre bridging is dependent on the design of the individual specimen and processing conditions such as fibre coating and a large scatter in propagation energy values can be found for tests performed on the same material[12]. Mode II fibre failures result from fibres fractured either in tension or compression[13].

The energy dissipation during delamination consists of resin deformation, microcracking, fibre pull-out and subsequent breakage. Their relative contributions to the toughness depend on the fibre/matrix interfacial strength which controls the amount of debonding[11]. Friedrich[14] suggested the following principle micromechanisms for energy absorption; crack bridging by fibres or fibre bundles, fibre breakage from the bridging, formation of the fracture surface, formation of side cracks and finally plastic deformation and/or microcracking of matrix around the fibres.

A model for the variation of fracture toughness with resin toughness and thickness of the interlaminar resin layer was established by Bradley and Cohen[11]. For brittle matrices tested under Mode I conditions, interaction of the crack tip with the fibres increases the resistance to crack growth if the interface is stronger than the matrix and if the crack moves into the

resin rather than breaking the fibres. A thin resin layer between plies would give more fibre interaction and would result in a higher toughness than for neat resin. In mixed modes and mode II, microcracking and a more frequent fibre-crack interaction should cause an increase in toughness from the neat resin. In ductile resins a zone around the crack tip with plastic deformation and microcracking leads to high energy dissipation. When shear stresses are present this zone will increase in size. The fibres, however, reduce the extent of this damage zone. Fibre and crack tip interaction should give a small increase in toughness but there ought to be a net decrease compared to the neat resin toughness. A thicker inter-ply resin region would give a higher toughness. Experiments were carried out with unidirectional specimens of four different material systems to test the predictions of the model. G_c was studied with respect to the effects of the thickness of the resin rich region, resin ductility, interfacial strength and loading mode. The ductile resins exhibited a lower toughness as the resin rich layer decreased whilst for brittle resins an increase in the neat resin toughness was observed due to the addition of fibres. In-situ SEM showed that the damage zone in ductile resins was larger than the interlaminar region and in brittle resins the damage zone was localised around the crack tip. Hibbs and Bradley[15] observed the size of the damage zone in ductile resins to be 8-10 fibre diameters. The damage zone around the crack tip is significantly larger in fatigue than in static loading[16] and the fatigue life of composites seems to be determined by a critical amount of damage such as debonding and sub-microscopic cracks rather than crack initiation and growth from defects[17]. Under a certain threshold strain energy release rate, G_{th}, no fatigue crack growth is observed[18].

The relationship between neat resin toughness and composite toughness was studied by Bradley[19]. The composite mode II toughness varied less with the neat resin toughness than did the composite mode I toughness. By increasing the ductility and reducing the yield

strength of the matrix, the delamination toughness increased because of a larger plastic zone ahead of the crack tip which provided more blunting. However, in ductile resins the plastic zone was truncated by the presence of the fibres which reduced the amount of load redistribution. The maximum toughness was achieved when no low energy fibre/matrix interfacial debonding is present. An increased resin toughness did not necessarily mean a large increase in laminate toughness. Hibbs and Bradley[15] suggest three reasons for this: premature failure may occur due to a weak fibre/matrix interface, the fibres provide a constraint which changes the stress state and limits the ductility of the resin, and the fibres act as rigid fillers which reduce the volume of material available for deformation.

Static and fatigue loading (R = 0 and R = -1) of mode II delamination was used to evaluate the importance of shear reversal for four composites with different mode I toughnesses including AS1/3501-6 and AS4/PEEK[20]. A decreasing ratio of G_{IIc}/G_{Ic} was observed as the matrix toughness increased; this varied from 5.5 for AS1/3501-6 to just 1.2 for the AS4/PEEK composite. The authors concluded that the improved matrix toughness is less beneficial in mode II and that the effect is further reduced or eliminated in fatigue. Shear reversal had an accelerating effect on crack propagation. An increase in interfacial strength was recognised as the key to optimising the interlaminar fatigue properties.

Jordan and Bradley[21] suggest that the fracture toughness is a material property and is independent of stacking sequence provided that what they call far field damage is ignored. Far field damage is the viscoelastic deformation which occurs because of loading of the resin remote from the crack tip; this is responsible for the high apparent G_c values observed in fractures at angle ply interfaces (e.g. +45°/-45°). However, the opposite was concluded by Ye and Friedrich[22] who examined the mode I fracture toughness of unidirectional glass fibre

reinforced polypropylene laminates manufactured from commingled yarns. The interlaminar fracture toughness was seen to be a complex interaction of matrix, fibre properties and fibre geometry. Very large amounts of fibre bridging was observed due to the fibre architecture obtained from this particular manufacturing technique. The propagation energy, G_I, is a measure of the global energy contributions and may also be dependent on specimen geometry and crack opening displacement. Sun and Zheng[1] showed, by means of plate finite elements, that the crack front in DCB and ENF experiments is skewed and that the skewness depends on the stacking sequence. No skewness is expected for unidirectional and cross-ply laminates.

Mixed mode failure criteria

For mode I and mode II the fracture mechanics approach is straightforward and crack advance is presumed to occur when the strain energy release rate exceeds the critical values, i.e. G_{Ic} or G_{IIc}. The situation is more complex for mixed mode loading. It is difficult to estimate an interaction of the two modes and to derive a criterion from simple physical models. Partitioning of the applied load into mode I and II components is often the favoured route. Whitney[23] suggests that fracture characterisation should concentrate on pure mode I and II and that a linear criterion, eqn(1), for mixed mode failure should be used.

$$\frac{G_I}{G_{Ic}} + \frac{G_{II}}{G_{IIc}} = 1 \qquad (1)$$

Empirical constants (*m* and *n* in eqn (2)) are sometimes included in the mixed mode failure criteria[24] to provide a better fit to experimental data.

$$(\frac{G_I}{G_{Ic}})^m + (\frac{G_{II}}{G_{IIc}})^n = 1 \quad (2)$$

A linear relationship between G_c, G_I and G_{II} has been observed[19]. Binienda et al.[25] suggest that G_I+G_{II} is constant for mixed modes with a ratio of $G_{II}/G_I<3$. For highly mode II dominated mixed modes, friction effects are important and lead to a high apparent fracture toughness. Wang et al.[26] observed that the critical energy release rate for mixed mode loading increases with an increasing mode II loading component. Failure loci have been established by Hashemi et al.[5,27] based on a critical crack opening displacement or with an interaction parameter, I_i, which varies linearly between 0 and 1 and is a function of the ratio of G_I/G, eqn(3).

$$(\frac{G_I}{G_{Ic}} - 1) \times (\frac{G_{II}}{G_{IIc}} - 1) \times I_i(\frac{G_I}{G_{Ic}}\frac{G_{II}}{G_{IIc}}) = 0 \quad (3)$$

Different failure criteria which take the appearance of the fracture surface into account have been developed. Such approaches ought to be more reasonable since they include actual physical considerations of the delamination micromechanisms. A general mixed mode criterion including a parameter ω to represent fracture surface roughness is shown in eqn(4). The surface roughness, which is 0° for smooth fracture surfaces, is material and fracture process dependent[28]. G_c is the measured fracture energy ($=G_I+G_{II}$), G_0 is the failure energy release rate, ψ is the phase angle of the applied loads and ψ_0 is the phase angle from the elastic mismatch across a bimaterial interface (i.e. a fibre/matrix interface). A good description of failure loci using this criterion for PEEK and epoxy composites has been obtained[29].

$$G_0 = G_c(\cos^2(\psi - \psi_0) + \sin^2\omega\ \sin^2(\psi - \psi_0)) \quad (4)$$

Hahn and Johannesson[30] proposed a model based on the fracture surface topography for the variation of G_c with the mode II component, eqn (5), where G' is the critical energy release rate due to fibre/matrix debonding, δ_m is the resin surface energy, v_f is the fibre volume fraction and K_I and K_{II} are the modes I and II stress intensity factors respectively. A modified version of this, eqn(6), has also been used[31], where E_L and E_T are the in-plane longitudinal and transverse Young's moduli respectively and c_1, c_2 and c_3 are empirical constants.

$$G_c = G' + 2\delta_m(1 - v_f)\sqrt{1 + (\frac{K_{II}}{K_I})^2} \quad (5)$$

$$G_c = G_I + G_{II} = -e^{-(c_1 M + c_2)} + c_3\ , \qquad M = \sqrt{1 + \frac{G_{II}}{G_I}\sqrt{\frac{E_L}{E_T}}} \quad (6)$$

More extensive reviews on fracture testing and failure criteria are available in Garg[32] and Reeder[33].

EXPERIMENTAL

Fracture toughness specimens were subjected to a fractographic examination following testing in a variety of loading modes. 3mm thick specimens were manufactured from 24-ply laminates with a stacking sequence of $(-45°, 0°, +45°)_{2S}(+45°, 0°, -45°)_{2S}$. As this is an anti-symmetric stacking sequence, the crack propagation is supposed to take place between a +45° and a -45° ply. The fibre/resin system was T300/914 which is carbon fibres in a poly(ether) sulfone modified epoxy resin. Non-adhesive Teflon inserts with a thickness of

about 50μm was used along the midplane to simulate a delamination. The DCB-specimens also had a Teflon edge delaminator to prevent any out-of-plane crack propagation. No specimens were precracked to simulate the midplane delamination.

The applied loading modes are listed in Table I together with the particular test methods that were used. For the fatigue tests, a load ratio of R=0.1 was used. The average fracture toughness propagation values for the different modes can be found in Table II. The mode I and II components have been calculated separately. The threshold values for fatigue crack propagation have also been identified where applicable and these were obtained from the sigmoidal Paris curves of da/dN versus G_{max} plotted on a log-log scale.

Table I. The different fracture modes examined within the present work and the respective methods used for fracture testing.

Mode	**Test method**
Mode I	DCB (Double Cantilever Beam)
Mixed mode I:II=6:1	MMB (Mixed Mode Bending)
Mixed mode I:II=4:3	FRMM (Fixed Ratio Mixed Mode)
Mixed mode I:II=3:4	MMB (Mixed Mode Bending)
Mixed mode I:II=3:10	MMB (Mixed Mode Bending)
Mode II	ELS (End Loaded Split)

Table II. The average propagation fracture toughnesses measured for the different modes. G_I, G_{II}, and G_{th} denote the mode I component, mode II component and fatigue threshold value respectively[34].

Mode	**G_I (J/m^2)**	**G_{II} (J/m^2)**	**G_{th} (J/m^2)**
Mode I	700	-	83
Mixed mode I:II=6:1	746.3	126.3	-
Mixed mode I:II=4:3	430	300	90
Mixed mode I:II=3:4	466.2	664.3	-
Mixed mode I:II=3:10	258.2	979	-
Mode II	-	1050	115.5

Fractography

Extensive details of the T300/914 system and its fractographic characteristics in different loading modes can be found in Gilchrist and Svensson[35]. The results from this previous work are summarised below.

The mode I fracture surface is best described by the general lack of cusps and by the large amount of fibre ends present. The pull-out is chiefly in bundles with the same amount on the opposing fracture surfaces, as shown in Fig. 1. The fibre/matrix interface is very strong since the pulled-out fibres all have a resin layer on them and all fibres have fractured very cleanly. Ridges and valleys, together with very little pull-out, mainly in the form of single fibres, and a general flat appearance are the characteristics for a mixed mode fracture surface with about equal mode I and II components, shown typically in Fig. 2. According to Purslow[36], ridges and valleys form under a combination of peel and shear stresses. Singh and Partridge[37] reported that the matrix deformation in interleaved carbon fibre/epoxy laminates increased significantly with an increasing component of mode II loading.

Figure 1.

Figure 2.

The most important fractographic feature for characterisation of the delamination mode is the cusp. Cusps are features that are formed by microcracking in the matrix just ahead of the crack tip (cusps are also commonly known as hackles in the literature). The cusps are oriented perpendicular to the fibres, bent over along them and have a width that is approximately equal to the distance between the fibres, see Fig. 3. The slope of the cusps out of the fracture plane are the same all over any given fracture surface. The characteristics of a mode II fracture surface have been determined by the present authors to be few broken

fibres, a rough resin fracture, relatively clean fibres and more cusps than in any other mode, Fig. 3.

Figure 3.

Cusp angle

Using the theory of cusp formation suggested by several authors[15,36,38,39] as being due to the coalescence of brittle microcracks in the resin, an expression for the angle at which cusps are inclined to the fracture surface can be derived from the stress state, shown in Fig. 4, of a small interlaminar resin element just ahead of the crack tip.

Figure 4.

During delamination crack propagation, the interlaminar tensile stress, σ_z, corresponds to the mode I component and the shear stress, τ_{xz}, to mode II. Using Mohr's circle for principal stresses on a small matrix element just ahead of the crack tip the values of the cusp angle for the different mode mixes can be calculated. These are shown in the graph below:

Figure 5.

This predicts that no cusps are formed for pure mode I (i.e., $\theta=0°$) and that the cusp angle is greatest for pure mode II at $\theta=45°$. It is worth noting that if some non-zero component of σ_x stress is present the cusp angle would be predicted to be greater for the mixed mode ratios (by between 2-8%).

The cusp angle was measured by means of scanning electron micrographs from different areas of the various fracture surfaces in mode I, mode II and different mixed modes. This particular fibre/resin system is difficult to inspect using scanning electron microscopy because of the two phase microstructure of the resin which masks many of the fracture surface characteristics. The 977 epoxy resin features, for example, are particularly clear when examined using SEM. Another complicating factor is that the cusps do not show a great similarity with each other even under the same loading mode. Two methods have been used to quantify the cusp angle. The best consistency in measuring cusp angle appears to be achieved by using the slope of the cusp at about one third of its height[40]. The true cusp angle is calculated from the tilt angle (of the SEM) and the apparent cusp angle (as measured from a micrograph). Tilt angles greater than 70-75° degrees are difficult to use due to rapidly deteriorating resolution and poor contrast of the image. The cusp angle would, of course, be easier to measure at high magnifications (>3500×) but clear images at such magnifications were beyond the scope of the SEM used. The cusp angles for the different loading modes are presented in Table III.

Table III. Measured cusp angles for different modes as defined using the cusp slope method.

Mode	**Cusp angle**	**Std. Dev.**
Mixed mode I:II=6:1	37.2°	2.29
Mixed mode I:II=4:3	43.7°	3.30
Mixed mode I:II=3:4	41.6°	3.29
Mixed mode I:II=3:10	49.9°	4.10
Mode II	54.0°	7.50

The other measurement procedure, using an average angle, yielded more scatter in the data. Some features that looked vaguely like cusps were found at only two locations of all the mode I fracture surfaces; hence these were omitted. The error in measuring cusp angles was estimated to be roughly ±3°.

The experimentally measured cusp angles are greater than those theoretically calculated for all modes. The cusp angles are seen to increase with the component of mode II loading but the experimentally measured angles are all greater than those predicted by theory by approximately 10-15°. This deviation between theory and experiment is most likely to be due to cusp rotation caused by shear stresses just prior to microcrack coalescence as suggested by Hibbs and Bradley[15]. The standard deviation is greater in mode II and this may also be a consequence of this. If stresses in the x-direction are imposed by the test jig this will, as previously mentioned, yield a larger cusp angle.

Fibre pull-out

Another feature that is considered potentially useful for characterising the fracture surface is the number of fibre ends present. These originate from the fibre pull-out process during fracture. The pull-out ought to increase with the mode I component and the present investigation has tried to establish a relationship between loading mode and the number of fibre ends found on the fracture surface. For each mode the number of fibre ends was determined at different locations. 3×12 sites were examined on each sample at a magnification of 350× using 0° tilt angle. An average value from all the sites was then calculated and the results are shown in Table IV. No locations were examined close to the non-adhesive inserts since a fibre end density value associated with the actual propagation values of G was desired. No crack propagation was observed to occur out of the midplane (i.e., no crack branching was observed).

Table IV. The density of fibre ends found for the different loading modes.

Mode	**Density (No./mm^2)**

Mode I	93.0
Mixed mode I:II=6:1	17.3
Mixed mode I:II=4:3	30.5
Mixed mode I:II=3:4	4.4
Mixed mode I:II=3:10	1.1
Mode II	7.5

A rapid decrease in the number of broken fibres as the mode I loading component decreases is noticed. This indicates that an opening stress is necessary to cause fibre fracture. The fibre pull-out and subsequent fibre fractures contribute to the commonly observed R-curve, i.e. the fracture toughness initially increases with an increasing crack length until a steady state propagation is obtained. For the present material R-curve behaviour was seen for the mode I dominated failures but not for the mode II dominates failures. No observations of pure shear failure of fibres, as reported by Purslow[13,36], were made in the present investigation.

Fracture toughness

From the active processes around the crack tip, Friedrich[14] assumed that the fracture energy is proportional to the fracture surface profile, the size of the damage zone, the fracture energy of the matrix, and the matrix volume fraction, the energy for forming side cracks in the damage zone and the volume fraction of such side cracks, the energy for fibre debonding, fibre bridging and fibre fracture and the volume fractions of such fibres. Another suggestion for the delamination process was presented by Johannesson et al.[38]. Fibres initially debond, probably due to stress concentrations at the interface, angled cracks are subsequently formed in the resin perpendicular to the major principal stress, and finally, the debonded regions and slant cracks are linked together by microscopic cracks propagating from the broken interfaces into the resin. Similar conclusions of the fracture processes that affect interlaminar fracture toughness are extensively available in the literature. In the present work, the effect of two of these processes have been examined, namely fibre pull-out and cusp formation.

Fig. 6 compares the variation of the experimentally determined cusp angle and mode II fracture toughness component as well as the theoretically predicted cusp angle with the loading mode. Qualitative agreement is evident which suggests that the formation of cusps at different angles, and hence the creation of different total fracture surface areas, directly influences the mode II fracture toughness during the steady state crack propagation.

Figure 6.

In a similar fashion, the variation of the amount of fibre pull-out and the mode I component of fracture toughness, both of which have been obtained experimentally, are compared in Fig. 7 against the loading mode. In this instance there is good qualitative agreement between the amount of fibre pull-out and the mode I toughness which suggests that the mechanism of fibre pull-out directly influences the dissipation of energy in a mode I manner.

Figure 7.

Failure criterion

The mixed mode failure criterion suggested by Charalambides et al.[28] was evaluated for the T300/914 material system using the fracture toughness values obtained by Osiyemi[34]. The criterion includes parameters such as the fracture surface roughness and the fibre/matrix interface fractures and good fits to experimental data have been reported[29]. The criterion is seen below together with the expressions for the four parameters. The values of these, Table V, were calculated from the fracture toughnesses given in Table II. The value for $G_{I/IIc}$, i.e., the fracture energy at $G_I=G_{II}$, was obtained from linear interpolation between the two adjacent mixed modes (i.e., mixed modes I:II=3:4 and I:II=4:3).

$$G_0 = G_c(\cos^2(\psi - \psi_0) + \sin^2\omega \sin^2(\psi - \psi_0))$$

where

$$G_0 = \frac{1}{1-\Omega^2}\left((\frac{G_{Ic} + G_{IIc}}{2}) - \sqrt{(\frac{G_{Ic} + G_{IIc}}{2})^2 - (1-\Omega^2)G_{Ic}G_{IIc}}\right)$$

$$\Omega = \frac{\sqrt{G_{Ic}G_{IIc}}}{2}(\frac{2}{G_{I/IIc}} - \frac{1}{G_{Ic}} - \frac{1}{G_{IIc}})$$

$$\tan^2\psi_0 = \frac{1-\frac{G_0}{G_{Ic}}}{1-\frac{G_0}{G_{IIc}}}$$

$$\tan^2\psi = \frac{G_{II}}{G_I}$$

$$\sin^2\omega = (\frac{G_0}{G_{Ic}} + \frac{G_0}{G_{IIc}}) - 1$$

Table V. The numerical values calculated for the parameters of the fracture criterion[28].

Parameter	Value
G_o	687.2 J/m^2
ω	52.9°
ψ_o	11.6°

Using the above equations, the parameter, ω, 'slope of the fracture surface roughness', was determined to be 52.9°, which is very close to the experimentally determined mode II cusp angle of 54.0°. This could be coincidental but Charalambides et al.[28] suggested that the surface roughness may well reflect the slope of microcracks formed ahead of the crack front, i.e., the cusp angle. Kinloch et al.[29] determined ω to be 41° for a carbon fibre/epoxy composite, 50° for a carbon fibre/PEEK composite at initiation and 41° for propagation. In the study by Charalambides et al.[28], ω-values of 44° and 46° were seen for the epoxy and PEEK systems respectively.

The fracture toughness, as determined experimentally and by the Charalambides criterion[28], was plotted to obtain the failure loci, Fig. 8. As can be seen from the graph the criterion only gives a good correlation with experiment for the pure mode I and II tests and the mixed mode I:II=4:3 test (FRMM); inferior agreement is obtained from the results of the MMB test procedure. Since the cusp angle has been seen to vary for the different loading modes a modification to the failure criterion is suggested that accounts for this. Assuming that the ω-parameter is the actual cusp angle and using the experimentally determined cusp angles, the failure locus will change in accordance with the dashed line in Fig. 8. The modified criterion gives a peak around mixed mode ratio I:II=1:1 which agrees well with observations by Reeder[33] who reported that fracture toughness data of epoxy composites reach a peak at this ratio. The fit to experimental fracture toughness data is better for the modified criterion than for the original criterion.

Figure 8.

DISCUSSION

SEM fractography of T300/914 is difficult due to the two phase structure of the resin which effectively obscures most of the features described in previous fractographic work. Some constraints have also been imposed on the present work by the inability to obtain sufficient resolution at higher magnifications (>3500×) with the particular SEM that was used.

The amount of fibre ends on the fracture surface was investigated for all modes. The general trend is that the fibre end density decreases rapidly from pure mode I to mode II dominated modes. The different values for static mixed mode I:II=4:3 may be due to the fact that another test configuration was used for the testing (i.e., MMB vs. FRMM). Thesken et al.[41] used an MMB rig to study delamination growth in carbon fibre/epoxy laminates and reported a substantial decrease in fibre bridging when a mode II loading component was present. As the amount of fibre pull-out is dependent on specimen and material parameters[10,12,14] this method of characterisation for different modes cannot be reliably used. From the results of the examination of this particular fibre/resin system, however, a very large number of broken fibres seems to be characteristic of mode I dominated fracture. The fact the no R-curve behaviour was seen for the mode II dominated fracture supports this.

Greenhalgh[40] reported an almost constant cusp angle for the mode I dominated mixed modes which then increased rapidly for highly mode II dominated failures. From similar observations[15,38,42,43,44] of the cusp angle changing with the mode of loading and the results of the present study, it seems likely that the cusp angle can be used to determine the fracture mode with confidence as was done by Gilchrist et al.[45] in the investigation of failure modes in composite I-beams. Also the cusp angles appear to be independent of the actual material system which supports the theory for microcrack formation.

Reeder[33] observed different mixed mode responses from carbon fibre/epoxy composites and carbon fibre/PEEK composites and concluded that no failure criterion based on just pure mode toughnesses would be able to fully predict the mixed mode behaviour of all materials. Mixed mode failure commonly occurs in actual engineering components and structures and hence it is important that mixed mode toughness testing is included in material characterisation. The MMB test method is well suited for this[44].

The modification of the failure criterion gives a better fit to experimental data for this particular material system. It also invokes a coupling to a physical process involved in the delamination fracture. The criterion will be further evaluated against experimental data from glass fibre/poly(ethylene) terephthalate. This work is currently in progress by the authors. The formation of cusps in thermoplastic systems ought also to be investigated. No references have been found that describe cusp formation in a tough thermoplastic matrix.

CONCLUSIONS

The formation of cusps and the processes of fibre pull-out have been shown to contribute respectively to the mode II and mode I fracture toughness components of carbon fibre/epoxy (T300/914C) laminates with a stacking sequence of $(-45°, 0°, +45°)_{2S}(+45°, 0°, -45°)_{2S}$. The cusp angle increases with an increased mode II loading component from about 37° for mixed mode I:II=6:1 to 54° for pure mode II. These values are 10-15° greater than those predicted theoretically with the difference decreasing for higher cusp angles and this is attributed to cusp rotation. The best consistency is obtained from measurements of the slope at a point some distance up the cusp rather than average cusp angle. There are significantly more cusps in the mode II dominated fractures than in mode I fractures. The cusp angle is the most

reliable method of determining the fracture mode. Fibre pull-out on its own can only be used to distinguish a highly mode I dominated fracture surface. Further indications of a particular mode of fracture are acquired from ridge and valley markings and the overall surface appearance.

The mixed mode fracture criterion of Charalambides et al.[28] was examined using the experimental results of the present investigation. Reasonable qualitative agreement was found, particularly for pure mode I and II results and the mixed mode I:II=4:3 results using the FRMM test procedure. A poorer agreement, however, was obtained for mixed mode results associated with the MMB test procedure and further studies are required to identify the reasons for this. The criterion was subsequently modified by replacing the surface roughness parameter with the experimental values for the cusp angle. This modification provided superior qualitative agreement between the failure criterion and the experimental fracture toughness data.

ACKNOWLEDGEMENTS

The authors would like to thank The Swedish Institute, The Marcus Wallenberg Foundation for Advanced Education in International Entrepreneurship and the International Collaboration Scheme of Forbairt for providing financial support. The support provided to M.D.G. by University College Dublin, by way of a President's Research Award, is also acknowledged. The help from Mr. Emile Greenhalgh, DRA, the staff at the Centre for Composite Materials, Imperial College, London and the Swedish Institute for Fibre and Polymer Fracture and the useful discussions with Professors J.G. Williams and A.J. Kinloch, both of Imperial College, London, are much appreciated.

REFERENCES

1. Sun, C.T. and Zheng, S., 'Delamination Characteristics of Double Cantilever Beam and End-Notched Flexure Composite Specimens.', *Composites Science and Technology*, **56**, 451-459 (1996).
2. Whitney, J.M., Browning, D.E. and Hoogesteden, W., 'A double cantilever beam test for characterizing Mode I delamination of composite materials.', *Journal of Reinforced Plastics and Composites*, **1**, 297-313 (1982).
3. Hashemi, S., Kinloch, A.J. and Williams, J.G., 'The analysis of interlaminar fracture in uniaxial fibre-polymer composites.', *Proceedings*, Royal Society, **A427**, 173-199, 1990.
4. Hashemi, S., Kinloch, A.J. and Williams, J.G., 'The Effects of Geometry, Rate and Temperature on the Mode I, Mode II and Mixed-Mode I/II Interlaminar Fracture of Carbon-Fibre/Poly(ether-ether ketone) Composites.', *Journal of Composite Materials*, **24**, 918-956 (1990).
5. Hashemi, S., Kinloch, A.J. and Williams, J.G., 'Mixed-Mode Fracture in Fibre-Polymer Composite Laminates.', *Composite Materials: Fatigue and Fracture (Third Volume), ASTM STP 1110*, American Society for Testing and Materials, 143-168, 1991.
6. Reeder, J.D. and Crews, J.H., Jr, 'Non-linear analysis and redesign of the mixed mode bending delamination test.', *NASA Technical Memorandum 102777*, 1991.
7. Harris, B., Dorey, S.E. and Cooke, R.G., 'Strength and Toughness of Fibre Composites.', *Composites Science and Technology*, **31**, 121-141 (1988).
8. Wilkins, D.J., Eisenmann, J.S., Camin, R.A., Margolis, W.S. and Benson, R.A., 'Characterizing Delamination Growth in Graphite-Epoxy.', *Damage in Composite Materials, ASTM STP 775*, American Society for Testing and Materials, 168-183, 1982.
9. Sato, N., Kurauchi, T. and Kamigaito, O., 'Fracture mechanisms of unidirectional carbon-fibre reinforced epoxy resin composite.', *Journal of Materials Science*, **21**, 1005-1010 (1986).
10. Hu, X.Z. and Mai, Y.W., 'Mode I Delamination and Fibre Bridging in Carbon-Fibre/Epoxy Composites With and Without PVAL Coating.', *Composites Science and Technology,* **46**, 147-156 (1993).
11. Bradley, W.L. and Cohen, R.N., 'Matrix Deformation and Fracture in Graphite-Reinforced Epoxies.', *Delamination and Debonding of Materials, ASTM STP 876*, American Society for Testing and Materials, 389-410, 1985.
12. Olsson, R., 'Factors Influencing the Interlaminar Fracture Toughness and its Evaluation in Composites.', *FFA report FFA TN 1991-34, Stockholm*, Sweden, 1991.
13. Purslow, D., 'Some Fundamental Aspects of Composite Fractography.', *Royal Aircraft Establishment, Technical Report 81127,* 1981.
14. Friedrich, K., 'Fractographic Analysis of Polymer Composites.', *Application of Fracture Mechanics to Composite Materials*, Elsevier Science Publishers B.V., 1989.
15. Hibbs, M.F. and Bradley, W.L., 'Correlations Between Micromechanical Failure Processes and the Delamination Toughness of Graphite/Epoxy Systems.', *Fractography of Modern Engineering Materials: Composites and Metals, ASTM STP 948,* American Society for Testing and Materials, 68-97, 1987.
16. Marom, G., 'Environmental Effects on Fracture Mechanical Properties of Polymer Composites.', *Application of Fracture Mechanics to Composite Materials*, Elsevier Science Publishers B.V., 1989.
17. Richards-Frandsen, R. and Naerheim, Y., 'Fracture Morphology of Graphite/Epoxy Composites.', *Journal of Composite Materials*, **17**, 105-113 (1983).
18. Hiley, M.J. and Curtis, P.T., 'Mode II Damage Development in Carbon Fibre Reinforced Plastics.', *AGARD: 74th Structures and Materials Meeting, Patras,* Greece, 1992.
19. Bradley, W.L., 'Relationship of Matrix Toughness to Interlaminar Fracture Toughness.', *Application of Fracture Mechanics to Composite Materials*, Elsevier Science Publishers B.V., 1989.
20. Russell, A.J. and Street, K.N., 'The Effect of Matrix Toughness on Delamination: Static and Fatigue Fracture Under Mode II Shear Loading of Graphite Fibre Composites.', *Toughened Composites, ASTM STP 937,* American Society for Testing and Materials, 275-294, 1987.
21. Jordan, W.M. and Bradley, W.L., 'Micromechanisms of Fracture in Toughened Graphite-Epoxy Laminates.', *Toughened Composites, ASTM STP 937*, American Society for Testing and Materials, 95-114, 1987.
22. Ye, L. and Friedrich, K., 'Mode I Interlaminar Fracture of Co-mingled Yarn Based Glass/Polypropylene Composites.', *Composites Science and Technology*, **46**, 187-198 (1993).
23. Whitney, J.M., 'Experimental Characterisation of Delamination Fracture.', *Interlaminar Response of Composite Materials,* Elsevier Science Publishers, 1989.
24. Carlsson, L.A. and Gillespie, J.W., 'Mode-II Interlaminar Fracture of Composites.', *Application of Fracture Mechanics to Composite Materials*, Elsevier Science Publishers B.V., 1989.

25. Binienda, W., Wang, A.S.D., Zhong, Y. and Reddy, E.S., 'A Criterion for Mixed-Mode Matrix Cracking in Graphite-Epoxy Composites.', *Composite Materials: Testing and Design (Ninth Volume), ASTM STP 1059,* American Society for Testing and Materials, 287-300, 1990.
26. Wang, A.S.D., Kishore, N.N. and Feng, W.W., 'On Mixed Mode Fracture in Off-Axis Unidirectional Graphite-Epoxy Composites.', *Progress in Science and Engineering of Composites, Fourth International Conference on Composite Materials (ICCM-IV),* Tokyo, 1982.
27. Hashemi, S., Kinloch, A.J. and Williams, J.G., 'Interlaminar Fracture of Composite Materials.', *Proceedings of Sixth International Conference on Composite Materials (ICCM-VI) London*, Elsevier Applied Science Publishers Ltd, 1987.
28. Charalambides, M., Williams J.G., Kinloch, A.J. and Wang, Y., 'On the analysis of mixed-mode failure.', *International Journal of Fracture*, **54**, 269-291 (1992).
29. Kinloch, A.J., Wang, Y. Williams, J.G., and Yayla, P., 'The Mixed-Mode Delamination of Fibre-Composite Materials.', *Composites Science and Technology*, **47**, 225-237 (1993).
30. Hahn, H.T. and Johannesson, T., 'A Correlation Between Fracture Energy and Fracture morphology in Mixed-Mode Fracture of Composites.', *Mechanical Behaviour of Materials IV, Proceedings of the Fourth International Conference, Stockholm,* Sweden, Pergamon Press Ltd, 1984.
31. Donaldson, S.L., 'The Effect of Interlaminar Fracture Properties on the Delamination Buckling of Composite Laminates.', *Composites Science and Technology,* **28**, 33-44 (1987).
32. Garg, C., 'Delamination - A Damage Mode in Composite Structures.', *Engineering Fracture Mechanics*, **29**, 557-584 (1988).
33. Reeder, J.R., 'An Evaluation of Mixed-Mode Delamination Failure Criteria.', *NASA Technical Memorandum 104210,* 1992.
34. Osiyemi, S.O., Department of Mechanical Engineering, Imperial College, London, private communication, 1994.
35. Gilchrist, M.D. and Svensson, N., 'A Fractographic Analysis of Delamination Within Multidirectional Carbon/Epoxy Laminates.', *Composites Science and Technology*, **55**, 195-207 (1995).
36. Purslow, D., 'Matrix Fractography of Fibre-Epoxy Composites.', *Royal Aircraft Establishment, Technical Report 86046,* 1986.
37. Singh, S. and Partridge, I.K., 'Mixed-Mode Fracture in an Interleaved Carbon-Fibre/Epoxy Composite.', *Composites Science and Technology*, **55**, 319-327 (1995).
38. Johannesson, T., Sjöblom, P. and Seldén, R., 'The detailed structure of delamination fracture surfaces in graphite/epoxy laminates'., *Journal of Materials Science*, **19**, 1171-1177 (1984).
39. Piggot, M.R., 'A New Model for Interface Failure in Fibre-Reinforced Polymers.', *Composites Science and Technology*, **55**, 269-276 (1995).
40. Greenhalgh, E.S., Defence Research Agency, UK, private communication, 1994.
41. Thesken, J.C., Brandt, F. and Nilsson, S., 'Investigations of Delamination Growth Rates and Criticality Along Heterogeneous Interfaces.', *19th Congress of the International Council of Aeronautical Sciences, Anaheim,* USA, 1994.
42. Johannesson, T. and Blikstad, M., 'Fractography and Fracture Criteria of the Delamination Process.', *Delamination and Debonding of Materials, ASTM STP 876*, American Society for Testing and Materials, 1985.
43. Arcan, L., Arcan, M. and Daniel, I.M., 'SEM Fractography of Pure and Mixed-Mode Interlaminar Fractures in Graphite/Epoxy Composites.', *Fractography of Modern Engineering Materials: Composites and Metals, ASTM STP 948,* American Society for Testing and Materials, 1987.
44. Benzeggagh, M.L. and Kenane, M., 'Measurement of Mixed-Mode Delamination Fracture Toughness of Unidirectional Glass/Epoxy Composites with Mixed-Mode Bending Apparatus.', *Composites Science and Technology,* **56**, 439-449 (1996).
45. Gilchrist, M.D., Kinloch, A.J. and Matthews, F.L., 'Mechanical Performance of Carbon-Fibre and Glass-Fibre-Reinforced Epoxy I-Beams: II. Fractographic Failure Observations.', *Composites Science and Technology*, **56**, 1031-1045 (1996).

Figure 1. Extensive fibre pull-out on a mode I fracture surface.

Figure 2. The fracture surface from a mixed mode I:II=6:1 failure. Ridges and valleys, together with very little pull-out, mainly single fibres, and a general flat appearance are the main characteristics.

Figure 3. A micrograph showing large cusps from a pure mode II delamination. The micrograph also shows one of the steps taken when measuring the cusp angle.

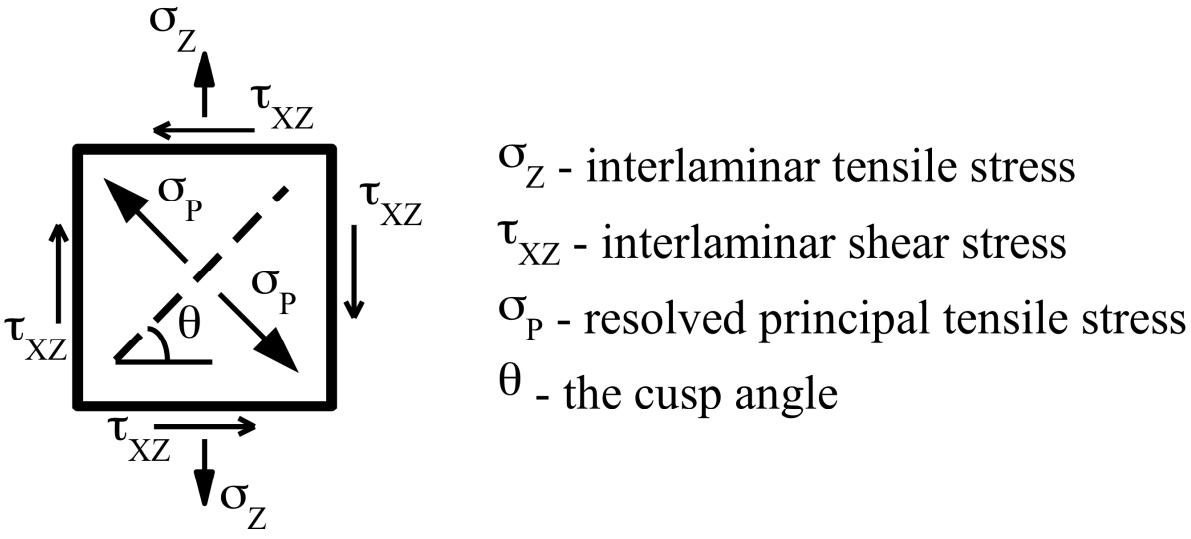

Figure 4. The stresses acting on a small resin element just ahead of the crack tip. The interlaminar tensile stress corresponds to the mode I component and the shear stress to the mode II component of load.

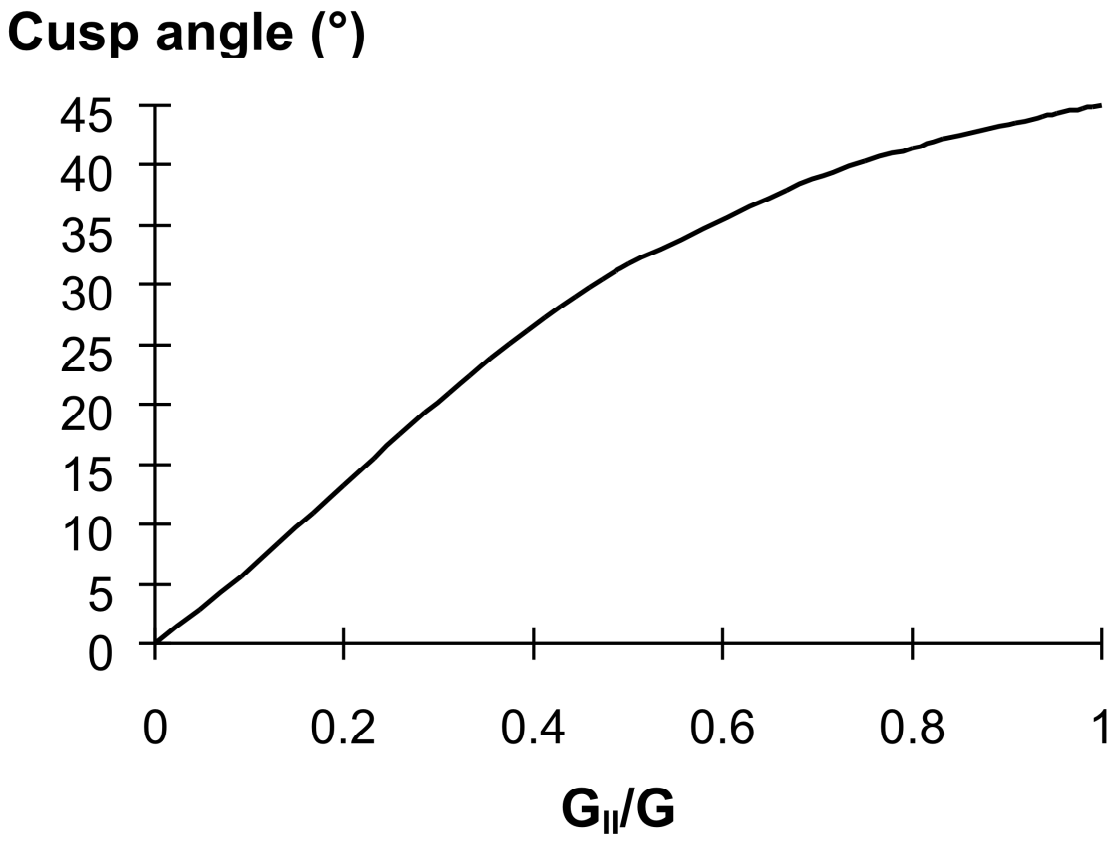

Figure 5. The theoretically predicted cusp angles as a function of the loading mode.

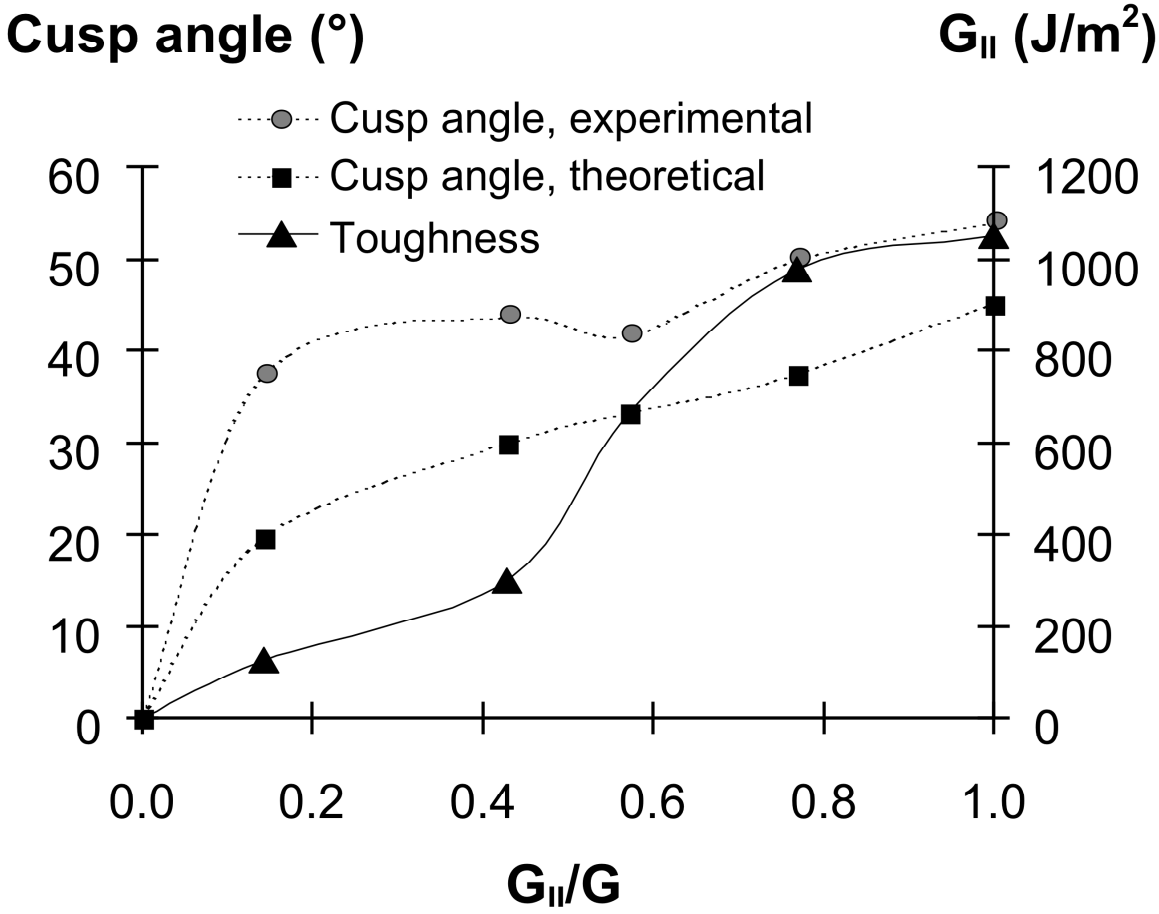

Figure 6. The experimentally determined cusp angle and the theoretically predicted cusp angle plotted together with G_{II} against the loading mode.

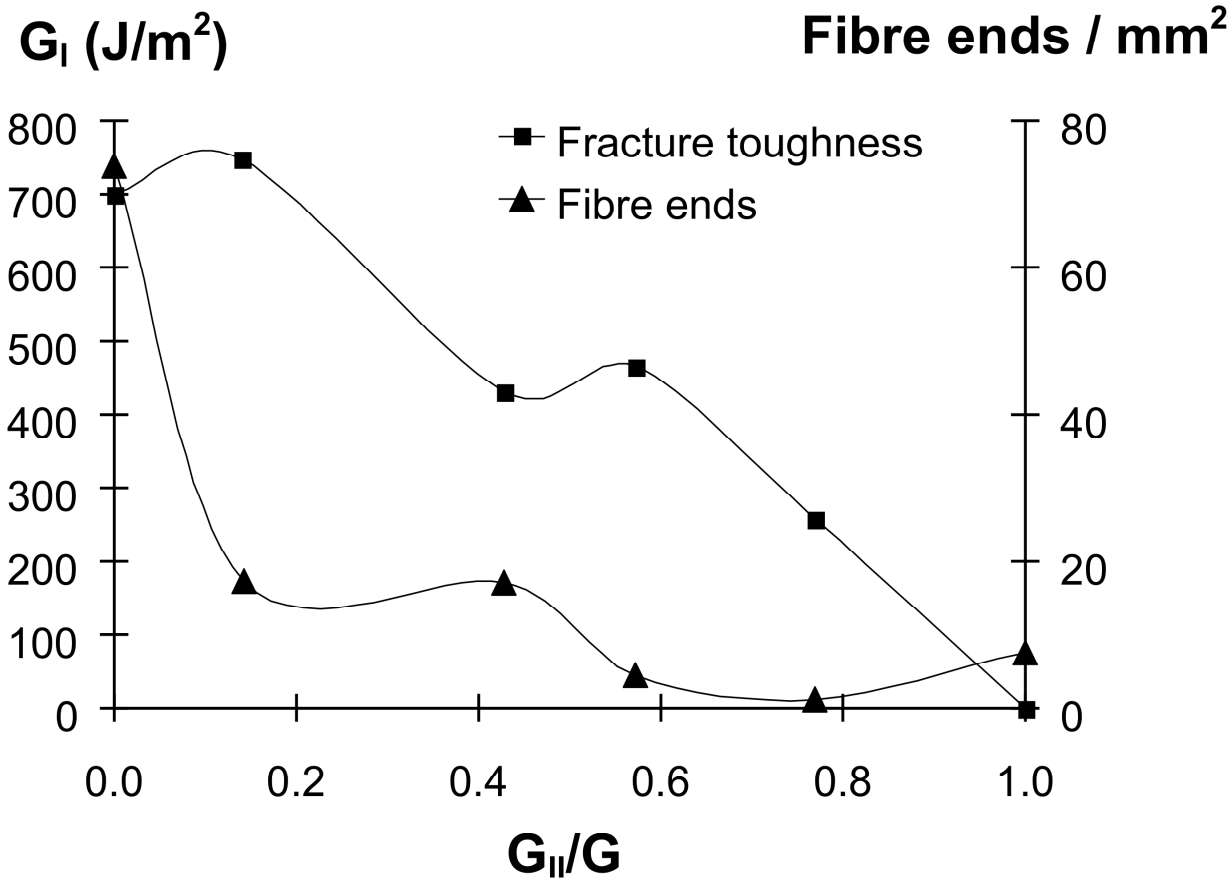

Figure 7. G_I and the amount of fibre ends on the fracture surface plotted for the different loading modes.

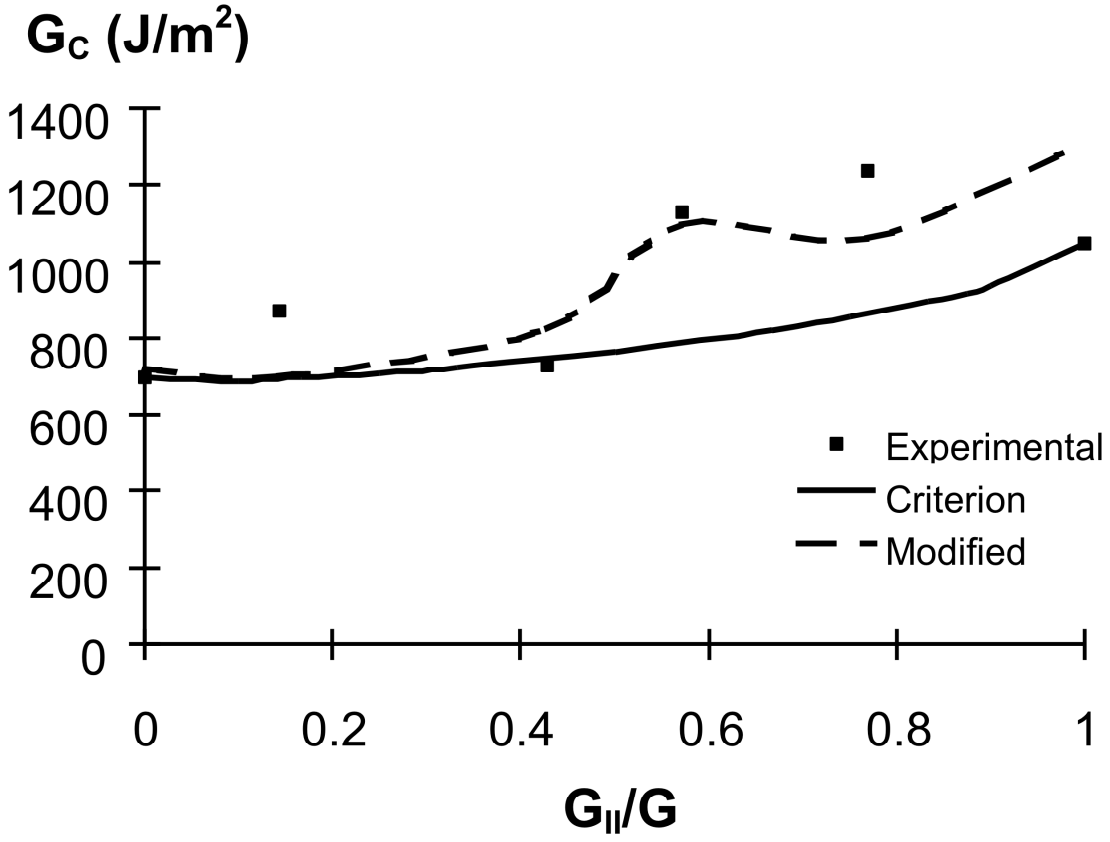

Figure 8. The experimental fracture toughness values, the failure loci for the Charalambides[28] criterion, eqn (4), and a modification to this criterion using experimentally determined cusp angles.